# Chiroptical signal enhancement in quasi-null-polarization-detection geometry: Intrinsic limitations

Hanju Rhee,[1,*] Intae Eom,[2] Sung-Hyun Ahn,[1] Ki-Hee Song,[1] and Minhaeng Cho[3,4,†]

[1]*Space-Time Resolved Molecular Imaging Research Team, Korea Basic Science Institute, Seoul 136-713, Korea*

[2]*Pohang Accelerator Laboratory, Pohang 790-834, Korea*

[3]*Center for Molecular Spectroscopy and Dynamics, Institute for Basic Science (IBS), Seoul 136-701, Korea*

[4]*Department of Chemistry, Korea University, Seoul 136-701, Korea*

(Received 14 February 2015; published 21 May 2015)

Despite its unique capability of distinguishing molecular handedness, chiroptical spectroscopy suffers from the weak-signal problem, which has restricted more extensive applications. The quasi-null-polarization-detection (QNPD) method has been shown to be useful for enhancing the chiroptical signal. Here, the underlying enhancement mechanism in the QNPD method combined with a heterodyne detection scheme is elucidated. It is experimentally demonstrated that the optical rotatory dispersion signal can be amplified by a factor of ∼400, which is the maximum enhancement effect achievable with our femtosecond laser setup. The upper limit of the QNPD enhancement effect of chiroptical measurements could, in practice, be limited by imperfection of the polarizer and finite detection sensitivity. However, we show that there exists an intrinsic limit in the enhancement with the QNPD method due to the weak but finite contribution from the homodyne chiroptical signal. This is experimentally verified by measuring the optical rotation of linearly polarized light with the QNPD scheme. We further provide discussions on the connection between this intrinsic limitation in the QNPD scheme for enhanced detection of weak chiroptical signals and those in optical enantioselectivity and Raman optical activity with a structured chiral field. We anticipate that the present work could be useful in further developing time-resolved nonlinear chiroptical spectroscopy.

DOI: 10.1103/PhysRevA.91.053839 PACS number(s): 33.55.+b, 42.25.Ja, 78.20.Ek

## I. INTRODUCTION

Optical activity resulting from the differential interaction of left- and right-circularly-polarized (LCP and RCP) beams is a property shown only by *chiral matter* with broken mirror symmetry [1]. Because of its unique ability to characterize the handedness of chiral species, chiroptical spectroscopy measuring frequency-dependent optical activity such as circular dichroism (CD), optical rotatory dispersion (ORD), and Raman optical activity (ROA), has widely been used in diverse research areas to determine stereospecific structures of chiral molecules [1–3]. However, most of the chiroptical methods suffer from the weakness of the corresponding signals imposed by weak magnetic dipole or electric quadrupole interaction-induced transitions. Enhancement of the chiroptical signal would thus enable extensive applications requiring high sensitivity, such as time-resolved chiroptical spectroscopy and microscopy.

The main difficulty of measuring a weak chiroptical signal in the conventional method utilizing LCP and RCP beams comes from a huge background contribution of the achiral signal, which is about four to six orders of magnitude larger than the chiral signal. Effective elimination or reduction of the achiral background is therefore essential to boost up the chiroptical measurement sensitivity. Pioneering work on enhancing chiroptical measurement has been done by Kliger and co-workers, who used an ellipsometric technique and its modified version to carry out nanosecond electronic CD and ORD experiments with significant signal enhancement in the UV-visible frequency range [4–6]. Instead of LCP and RCP light, a pair of elliptically (rotated linearly) polarized beams were used as incident radiation for CD (ORD) measurements in their setup. Similar approaches have been applied in the IR frequency range as well to measure vibrational CD and ORD signals that are much weaker than the electronic ones [7]. Recently, interesting alternatives measuring wave interference between a chiral signal and a reference field called a *local oscillator* (LO) have been developed for electronic and vibrational CD and ORD [8–11], and nonlinear coherent anti-Stokes Raman scattering ROA (CARS-ROA) measurements [12,13].

A key ingredient commonly used for chiroptical enhancement in the above methods is *quasi-null-polarization detection* (QNPD), where the incident and detection polarizations are properly controlled such that the chiral signal remains constant while the achiral signal decreases. Thereby, the ratio of chiral to achiral signal, which is related to the chiroptical enhancement factor, can be significantly increased even though the total signal (chiral+achiral) actually decreases. However, such an enhancement effect is limited not only because the total amount of photons detected decreases as the achiral signal approaches zero, but also because the cross term of the chiral and achiral signals vanishes so that phase (sign) information that is a characteristic property of the chiral signal is lost. In this case, the enhancement effect cancels out or even gets worse, which implies that there exists an explicit limit for the maximum enhancement that is theoretically or experimentally possible [14,15]. There still remain questions about how much enhancement could be achieved and which factor would determine its upper limit in the QNPD method.

In this paper, we address chiroptical signal enhancement in the QNPD method. First, a brief account of the close relation between chiroptical measurement and heterodyned detection is presented. Then we describe the chiroptical enhancement mechanism of the QNPD method on the basis of a heterodyned detection scheme and demonstrate that there

*Corresponding authors: hjrhee@kbsi.re.kr

†mcho@korea.ac.kr

 

exists an intrinsic upper limit of the chiroptical enhancement in the QNPD method using both simulation and experiment. Other practical issues influencing the enhancement factor such as imperfections of real polarizers and detector sensitivity are also discussed, and a range of future applications are briefly noted.

## II. THEORY

Typically, the electronic chiroptical transition intensity is two to three orders of magnitude smaller than the absorption at visible wavelengths, since the molecular dimension is smaller than the wavelength of chiral light. For vibrational optical activity (VOA), the relative chiroptical intensity compared to the absorption is further reduced to $10^{-4}$–$10^{-6}$ not only because the IR wavelength is an order of magnitude larger than the visible but also because the effective radius ($r$) of charge circulation by nuclear vibration is much smaller than that by the more delocalized electronic state. Therefore, there is a great need for significant enhancement of the VOA signal in the IR frequency range [16].

### A. Chiroptical effect on an electric field

Within the linear response theory, the transmitted electric field vector through a solution containing chiral molecules can be written as

$$|\Psi\rangle = e^{-i\hat{A}_c L}|\psi\rangle, \tag{1}$$

where $|\psi\rangle$ is the incident electric field vector, and the operator $\hat{A}_c$ representing the weak chiroptical effects on the propagating light is given as

$$\hat{A}_c = \left(\rho - \frac{i\kappa}{2}\right)\hat{I} - \left(\frac{\delta}{2} - \frac{i\eta}{4}\right)\hat{\sigma}_y. \tag{2}$$

Here, $\hat{I}$ and $\hat{\sigma}_y$ are the 2×2 identity matrix and the $y$-component vector of the Pauli matrices, respectively. $L$ is the thickness of the solution sample and $\kappa$, $\rho$, $\eta$, and $\delta$ are the absorption coefficient [$=(\ln 10)\varepsilon c$], dispersion ($=2\pi n/\lambda$), circular dichroism [$=\ln 10(\varepsilon_L - \varepsilon_R)c$], and circular birefringence [$=2\pi(n_L - n_R)/\lambda$], respectively, where $\varepsilon$, $n$, $\lambda$, and $c$ are, respectively, the decadic molar extinction coefficient, refractive index, wavelength, and molar concentration. Typically, the ratios $\eta/\kappa$ and $\delta/\rho$ are on the order of $|m/(\mu c)| \sim 10^{-3}$–$10^{-2}$, where $m$ and $\mu$ represent the transition magnetic and electric dipoles of a chiral molecule.

Now, the chiral-medium influence operator $e^{-i\hat{A}_c L}$ can be rewritten as

$$e^{-i\hat{A}_c L} = e^{-\kappa L/2 - i\rho L}\begin{pmatrix}\cosh x & -i\sinh x \\ i\sinh x & \cosh x\end{pmatrix}, \tag{3}$$

where

$$x = \frac{\eta L}{4} + \frac{i\delta L}{2}. \tag{4}$$

Note that the real and imaginary parts of $x$ are related to the CD and circular birefringence (or ORD). We shall consider two specific cases where the incident light is either elliptically polarized or rotated linearly polarized, which have been used to measure the CD and ORD dissymmetry factors, respectively.

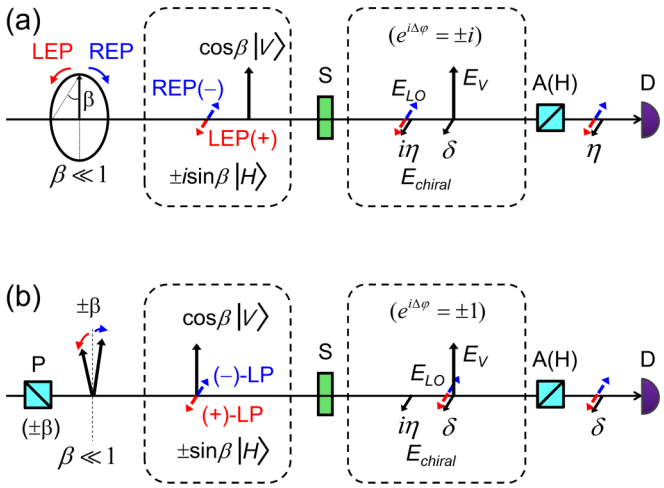


FIG. 1. (Color online) QNPD optical schemes for (a) CD and (b) ORD signal enhancement. Instead of LCP and RCP or (±45°)-rotated LP, LEP and REP with a small ellipticity of $\beta$ (a) or (±)-LP beams slightly rotated by $\beta$ (b) are used as incident radiation. P, polarizer; S, chiral sample; A, analyzer; D, detector. The analyzer (A) allows only the horizontal field ($E_{\text{chiral}} + E_{\text{LO}}$) to be transmitted through while the vertical field ($E_V$) is blocked. Note that the phase differences ($\Delta\varphi$) between $E_V$ and $E_{\text{LO}}$ are ±90° for (a) CD and 0° or 180° for (b) ORD.

### B. CD measurement with elliptically polarized light

Now, let us consider the experimental configuration [see Fig. 1(a)] that involves incident left (+) and right (−) elliptically polarized (LEP and REP) light which is written as a linear combination of the two basis polarization states, i.e.,

$$|\psi^{\pm}\rangle = \cos\theta|V\rangle \pm i\sin\theta|H\rangle, \tag{5}$$

where $|V\rangle$and $|H\rangle$ are the vertical and horizontal polarization states, respectively.

In the present QNPD scheme, the incident elliptically polarized light (EPL) is controlled to be weakly elliptical [see Eq. (5)] and the major axis of the polarization ellipse is assumed to be parallel to $|V\rangle$. Then, only the horizontal component of the transmitted field is allowed to pass through the linear polarizer placed in front of the photon detector, so that we need to consider the $|H\rangle$-projected component of $|\Psi^{\pm}\rangle$,

$$\begin{aligned} E_H^{\pm} &= \langle H|\Psi^{\pm}\rangle = \langle H|e^{-i\hat{A}_c L}|\psi^{\pm}\rangle \\ &= e^{-\kappa L/2 - i\rho L}(i\cos\theta\sinh x \pm i\sin\theta\cosh x) \\ &= e^{-\kappa L/2 - i\rho L}\left(i|E_V^0|\sinh x \pm i|E_H^0|\cosh x\right), \end{aligned} \tag{6}$$

where the electric field amplitudes of the vertical and horizontal components of the incident EPL are denoted as $|E_V^0|$ ($=|\langle V|\psi^{\pm}\rangle|$) and $|E_H^0|$ ($=|\langle H|\psi^{\pm}\rangle|$), respectively. Note that the horizontal component of the transmitted $E$ field consists of two contributions. The first term in Eq. (6) is produced by the interaction of the vertical (major) component of the incident EPL with chiral molecules, which makes $E_V^0$ rotate via the ORD effect and change its polarization state to become elliptically polarized with a nonzero $H$ component via the CD effect. Now, the second term in Eq. (6) originates from the $H$

component of the incident EPL whose phase and amplitude are altered by its interaction with chiral molecules.

In general, due to the weakness of chiroptical effects, i.e., $|\eta|L/4 \ll 1$ and $|\delta|L/2 \ll 1$, we have $|x| \ll 1$. Therefore, Eq. (6) can be approximately written as

$$E_H^{\pm} = ie^{-\kappa L/2 - i\rho L}\left(|E_V^0|\left\{\frac{\eta L}{4} + \frac{i\delta L}{2}\right\} \pm |E_H^0|\right). \quad (7)$$

Note that the first term in Eq. (7) is directly related to the CD ($\eta$) and circular birefringence ($\delta$), whereas the second term is just the attenuated and dispersed component resulting from the H component of the incident EPL. From Eq. (7), one can immediately find that the H component of the incident EPL (the second term) behaves like a local oscillator (or reference) field that interferes with the chiroptical signal field (the first term). Therefore, we shall introduce notations to refer to these two contributions as

$$\begin{aligned} E_{\text{chiral}} &= ie^{-\kappa L/2 - i\rho L}|E_V^0|\sinh x \\ &\cong ie^{-\kappa L/2 - i\rho L}\left(\frac{\eta L}{4} + \frac{i\delta L}{2}\right)|E_V^0| \end{aligned} \quad (8)$$

and

$$E_{\text{LO}} = ie^{-\kappa L/2 - i\rho L}|E_H^0|\cosh x \cong ie^{-\kappa L/2 - i\rho L}|E_H^0|, \quad (9)$$

so that Eq. (7) is rewritten as

$$E_H^{\pm} = E_{\text{chiral}} \pm E_{\text{LO}}. \quad (10)$$

As can be seen in Eqs. (8) and (9), the CD contribution ($\propto\eta$) to the chiral field is either in or out of phase with the local oscillator, depending on the sign of $\eta$, whereas the ORD contribution ($\propto\delta$) is in quadrature ($\pm 90°$) with the LO.

As shown in Fig. 1(a), the transmission axis of the analyzer is aligned perpendicular to the major axis of the incident EPL so that the detector (D) reads only the horizontal components as

$$\begin{aligned} I^{\pm} &= |E_{\text{chiral}} \pm E_{\text{LO}}|^2 \\ &= |E_{\text{chiral}}|^2 + |E_{\text{LO}}|^2 \pm 2\text{Re}[E_{\text{chiral}}E_{\text{LO}}^*], \end{aligned} \quad (11)$$

where $I^{\pm}$ is the transmitted intensity for LCP (+) and RCP (−) beams [or (±)-rotated linearly polarized (LP) beams for ORD measurement] in the present QNPD geometry. Equation (11) consists of the molecular-chirality-independent homodyne term $I_{\text{homodyne}} = |E_{\text{chiral}}|^2 + |E_{\text{LO}}|^2$, and the chirality-sensitive heterodyne (interference) term $I_{\text{heterodyne}} = 2\text{Re}[E_{\text{chiral}}E_{\text{LO}}^*]$. The CD signal or dissymmetry factor ($g$) is given as the intensity difference between LCP and RCP beams normalized by their average intensity,

$$g = \frac{I^+ - I^-}{(I^+ + I^-)/2} = \frac{2I_{\text{heterodyne}}}{I_{\text{homodyne}}} = \frac{4\text{Re}[E_{\text{chiral}}E_{\text{LO}}^*]}{|E_{\text{chiral}}|^2 + |E_{\text{LO}}|^2}. \quad (12)$$

Equations (11) and (12) show that the CD signal ($g$) is essentially the ratio of the heterodyne (interference) to the homodyne signals. Note that the phase information about the complex $E_{\text{chiral}}$ is obtained only from the heterodyne term ($2\text{Re}[E_{\text{chiral}}E_{\text{LO}}^*]$) while the homodyne one ($|E_{\text{chiral}}|^2 + |E_{\text{LO}}|^2$) contributes to the detected field intensities $I^{\pm}$ as a positive background.

Inserting Eqs. (8) and (9) into Eq. (12), we find that

$$\begin{aligned} g &= \frac{4\text{Re}[\sinh x\ \cosh x^*]|E_V^0||E_H^0|}{|\sinh x|^2|E_V^0|^2 + |\cosh x|^2|E_H^0|^2} \cong \frac{4\text{Re}[x]|E_V^0||E_H^0|}{|x|^2|E_V^0|^2 + |E_H^0|^2} \\ &= 4\text{Re}[x]\frac{\beta}{\beta^2 + |x|^2}, \end{aligned} \quad (13)$$

where the second approximate equality was obtained from $|x| \ll 1$ and the aspect ratio $\beta$ of the incident EPL is related to its ellipticity angle $\theta$ as

$$\beta = \frac{|E_H^0|}{|E_V^0|} = \frac{\sin\theta}{\cos\theta}. \quad (14)$$

At small ellipticity angle, i.e., weakly elliptically polarized light, the aspect ratio is approximately identical to the ellipticity angle, i.e., $\beta \cong \theta$.

To show the enhancement effect of the QNPD method on the CD signal ($g$), let us consider the standard case that the incident light beams used are left and right circularly polarized light (CPL) ($\theta = \pm 45°$) that form the complete set of basis states. Then the dissymmetry factor for CD in this case is given as

$$g_{\text{CPL}} = \frac{4\text{Re}[x]}{1 + |x|^2}. \quad (15)$$

Therefore, we now introduce the enhancement factor $G$ defined as the ratio of $g$ to $g_{\text{CPL}}$, that is,

$$G = \frac{g}{g_{\text{CPL}}} = \frac{\beta(1 + |x|^2)}{\beta^2 + |x|^2}. \quad (16)$$

Note that the aspect ratio $\beta$ is what one can easily control experimentally. In the case that $\beta \gg |x|$, the chiral signal amplitude is much smaller than the LO amplitude, i.e., $|E_{\text{chiral}}| \ll |E_{\text{LO}}|$ and the enhancement factor is inversely proportional to the aspect ratio so that one can increase the $G$ factor by making the ellipticity of the EPL beams small. However, as the aspect ratio $\beta$ is further decreased below $|x|$, the chiral field amplitude becomes larger than the LO amplitude, i.e., $|E_{\text{chiral}}| > |E_{\text{LO}}|$ and the enhancement factor becomes linearly proportional to $\beta$ so that the enhancement effect in this domain disappears. From Eq. (16), one can immediately find that the enhancement factor $G$ and the dissymmetry factor $g$ have intrinsic upper limits at

$$\beta_{\max} = |x| = \sqrt{\left(\frac{\eta L}{4}\right)^2 + \left(\frac{\delta L}{2}\right)^2},$$

which are

$$G_{\max} = \frac{g(\beta_{\max})}{g_{\text{CPL}}} = \frac{(1 + |x|^2)}{2|x|} \quad (17)$$

and

$$g(\beta_{\max}) = \frac{2\text{Re}[x]}{|x|} = \frac{\eta/2}{\sqrt{(\eta/4)^2 + (\delta/2)^2}}. \quad (18)$$

Since the chiroptical effects are very weak, i.e., $|x| \ll 1$, the maximum enhancement factor ($\sim 1/2|x|$) is indeed very large.

### C. ORD measurement with slightly rotated linearly polarized light

Instead of using EPL, one can use slightly rotated linearly polarized light (LPL) beams to measure ORD signals, where the incident beam polarization states are

$$|\psi^{\pm}\rangle = \cos\phi|V\rangle \pm \sin\phi|H\rangle. \tag{19}$$

The rotation angle of LPL from the vertical direction is denoted as $\phi$. In the present QNPD scheme with incident rotated LPL beams [see Fig. 1(b)], the horizontal component of the transmitted field which is allowed to pass through the analyzer is found to be

$$\begin{aligned} E_H^{\pm} &= \langle H|\Psi^{\pm}\rangle = e^{-\kappa L/2 - i\rho L}(i\cos\phi\sinh x \pm \sin\phi\cosh x) \\ &= e^{-\kappa L/2 - i\rho L}\left(i\left|E_V^0\right|\sinh x \pm \left|E_H^0\right|\cosh x\right). \end{aligned} \tag{20}$$

Again, since the chiroptical effects are very weak, $|\eta|L/4 \ll 1$ and $|\delta|L/2 \ll 1$, we have

$$\begin{aligned} E_H^{\pm} &\cong e^{-\kappa L/2 - i\rho L}\left(i\left|E_V^0\right|\left\{\frac{\eta L}{4} + \frac{i\delta L}{2}\right\} \pm \left|E_H^0\right|\right) \\ &= E_{\text{chiral}} \pm E_{\text{LO}}, \end{aligned} \tag{21}$$

where the chiral and LO terms are given as

$$\begin{aligned} E_{\text{chiral}} &= ie^{-\kappa L/2 - i\rho L}\left|E_V^0\right|\sinh x \\ &\cong ie^{-\kappa L/2 - i\rho L}\left(\frac{\eta L}{4} + \frac{i\delta L}{2}\right)\left|E_V^0\right| \end{aligned} \tag{22}$$

and

$$E_{\text{LO}} = e^{-\kappa L/2 - i\rho L}\left|E_H^0\right|\cosh x \cong e^{-\kappa L/2 - i\rho L}\left|E_H^0\right|. \tag{23}$$

The only difference between the CD measurement with EPL beams and the ORD measurement with rotated LPL beams is the difference in the phases of the corresponding LO fields [compare Eq. (23) with Eq. (9)].

Now, the dissymmetry factor defined in Eq. (12) can be measured and it provides information on ORD as

$$\begin{aligned} g &= \frac{I^+ - I^-}{(I^+ + I^-)/2} = \frac{4\text{Re}[E_{\text{chiral}}E_{\text{LO}}^*]}{|E_{\text{chiral}}|^2 + |E_{\text{LO}}|^2} \\ &\cong 4\text{Im}[x]\frac{\beta}{\beta^2 + |x|^2}. \end{aligned} \tag{24}$$

The aspect ratio, $\beta$, in this case of the rotated LPL is related to its rotation angle $\phi$ as

$$\beta = \frac{\left|E_H^0\right|}{\left|E_V^0\right|} = \frac{\sin\phi}{\cos\phi}. \tag{25}$$

At small rotation angle, the aspect ratio approximately equals the rotation angle, i.e., $\beta \cong \phi$.

To show the QNPD enhancement effect on the ORD signal ($g$), we consider the cases that the incident LPL beams are rotated LPL with rotation angle $\phi = \pm 45°$——note that the two LPL beams correspond to the two orthogonal basis states. Then the dissymmetry factor for ORD in this case is given as

$$g_{45} = \frac{4\text{Im}[x]}{1 + |x|^2}. \tag{26}$$

The enhancement factor $G$ defined as the ratio of $g$ to $g_{45}$ is found to be identical to Eq. (16) except for the difference in the definition of the aspect ratio [compare Eq. (14) with Eq. (25)], i.e.,

$$G = \frac{g}{g_{45}} = \frac{\beta(1 + |x|^2)}{\beta^2 + |x|^2}. \tag{27}$$

Also, the intrinsic upper limits of the enhancement factor $G$ and the ORD dissymmetry factor $g$ are at

$$\beta_{\text{max}} = |x| = \sqrt{\left(\frac{\eta L}{4}\right)^2 + \left(\frac{\delta L}{2}\right)^2},$$

and they are

$$G_{\text{max}} = \frac{g(\beta_{\text{max}})}{g_{45}} = \frac{(1 + |x|^2)}{2|x|} \tag{28}$$

and

$$g(\beta_{\text{max}}) = \frac{2\text{Im}[x]}{|x|} = \frac{\delta}{\sqrt{(\eta/4)^2 + (\delta/2)^2}}. \tag{29}$$

Since $|x| \ll 1$, the maximum enhancement factor $G_{\text{max}}$ is again $\sim 1/2|x|$.

In this section, we have shown that the underlying mechanisms of the enhancement effects found in both the CD measurement with EPL beams [see Fig. 1(a)] and the ORD measurement with rotated LPL beams [see Fig. 1(b)] are essentially the same. Now, measuring the ORD signals for varying aspect ratio of the rotated LPL beams, we experimentally show that there is indeed an upper limit of the enhancement effect and further discuss its origin and connection to the intrinsic limit of optical enantioselectivity and the ROA signal with the structured or the so-called superchiral field.

## III. EXPERIMENTAL AND NUMERICAL SIMULATION METHODS

The experimental layout of the QNPD for ORD measurement is shown in Fig. 2. A femtosecond pulse train (Libra, Coherent Inc.) centered at 800 nm is used as incident light source and two polarizing components respectively as a polarization rotator (Glan-Laser polarizer, P) and an analyzer (Glan-Thomson polarizing beam splitter, PBS), in between which the chiral sample (CS) is placed. For ORD measurement, the transmission axis of the first polarizer (P) on a motorized rotational stage is slightly rotated left [(+)-LP] and right [(−)-LP] from the crossed angle position (vertical) with that of the analyzer (horizontal). Here, the PBS spatially separates the horizontally ($S_\perp$) and vertically ($S_\parallel$) emitted signal beams after the chiral sample. The $S_\perp$ corresponds

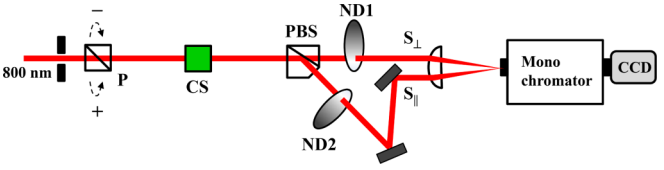


FIG. 2. (Color online) The experimental layout of the QNPD for ORD measurement. P, Glan-laser polarizer; PBS, Glan-Thomson polarizing beam splitter; CS, chiral sample; ND1 and ND 2, neutral density filters; CCD, charge-coupled device detector.

to the transmitted signal ($I^{\pm}$) described in the text, whereas the $S_{\|}$, which carries the achiral response signal, is used for correcting the intensity fluctuation of the light source (intensity referencing). These two beams are focused into the entrance slit of the monochromator; it is slightly displaced vertically and then detected in the lower and upper tracks of the CCD detector (PIXIS100B, Princeton Inst.), respectively. For calculating the dissymmetry factor ($g$), only the signals at a specified CCD pixel ($\lambda_{\rm det} = 800$ nm) were used. To gain statistical information (the standard deviation of the ORD signal), pulsed measurements (4000 shots for each $I^{\pm}$) were made by synchronizing the CCD with the 200 Hz laser repetition rate. Neutral density filters (ND1 and ND2) are used to avoid detector saturation as well as to examine the effect of the total amount of photons detected on the enhancement of the chiroptical signal (see the results in the next section for more detail).

The chiral sample used for the ORD measurement is Ni(+) $(\text{tartrate})_2$ in aqueous solution. The ORD signal of aqueous Ni(+) $(\text{tartrate})_2$ is large enough at 800 nm that the contribution of its homodyne signal intensity ($|E_{\rm chiral}|^2$) to the chiroptical enhancement can be readily measured experimentally [8]. Low (24 mM) and high (120 mM) concentrations of the sample were compared to investigate how the chiroptical enhancement effect is changed depending on the homodyne signal intensity.

For numerical simulation, Eqs. (11) and (24) were calculated considering only the shot noise of photons and the dark noise of the CCD without photons. The standard deviation of photon counts equals the square root of the average photon number ($N$) so that the signal-to-noise ratio (SNR) is given as $N/\sqrt{N} = \sqrt{N}$. Simulating each fluctuating intensity with dark and shot noises, the following stepwise procedure was used: First, the amplitudes of the chiral signal ($|E_{\rm chiral}| = |(\delta L/2)E_V^0|$) and LO ($|E_{\rm LO}| = |(\sin\beta)E_V^0|$) fields are calculated from a specified incident vertical field strength ($|E_V^0|$) and the Malus law, assuming that there is no attenuation of the incident beam by the sample absorption ($\eta = 0$), scattering, or any other reflections of the optics. Second, $I^{\pm}$ in Eq. (11) is then obtained from the calculated $|E_{\rm chiral}|$ and $|E_{\rm LO}|$. Last, the dark and shot noises are added to the average photon number $N$, assuming that $N$ is proportional to each intensity (the square of the electric field).

## IV. EXPERIMENTAL RESULTS

Figure 3 shows the ORD enhancement of aqueous Ni(+) $(\text{tartrate})_2$ solution (3 mM) measured in the QNPD scheme. In the cases that $\beta$ is relatively large (>0.002), the ORD signal (squares) increases and is simply proportional to $1/\beta$ (dashed line) as the incident rotation angle of the ($\pm$) LP beam decreases. In the region where $\beta < 0.002$ (see the inset of Fig. 3), however, the measured ORD enhancement effect decreases together with $\beta$. The enhancement effect is maximal at ~400 ($\beta = 1.7 \times 10^{-3}$). According to the theory discussed in the above section, the intrinsic maximum enhancement should be obtained as $G_{\rm max} \cong 1/2|x|$ at $\beta_{\rm max} = |x|$. Since the original ORD ($\delta L/2$) and CD ($\eta L/4$) signals at 3 mM are respectively $1.4 \times 10^{-4}$ rad and $-7.0 \times 10^{-5}$ rad ($|x| = 1.6 \times 10^{-4}$), one should theoretically have $G_{\rm max} = 3100$ at $\beta_{\rm max} = 1.6 \times 10^{-4}$, which is an order of magnitude larger (for $G_{\rm max}$) or smaller

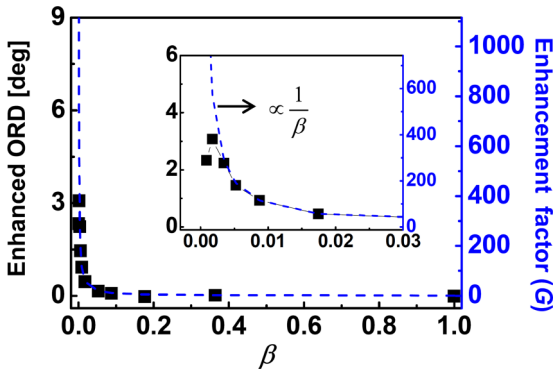


FIG. 3. (Color online) The enhanced ORD signal (squares) measured at 800 nm for 3 mM aqueous Ni(+) $(\text{tartrate})_2$. The enhancement is increased with the $1/\beta$ curve (dashed line) at large $\beta$ but decreases below $\beta = 0.002$ (inset).

(for $\beta_{\rm max}$) than the experimental result. This large difference between the experiment and the theory implies that there are other technical issues. For instance, real polarizers (P and PBS in Fig. 2) are not optically perfect and have limited extinction ratio (~$10^{-5}$). Consequently, a leakage transmitted through the analyzer (PBS) could interfere with the ORD signal, giving rise to an unfavorable enhancement at very small $\beta$.

In the present case where the original chiroptical strength is very small ($|x| = 1.6 \times 10^{-4}$), the technical problems caused by imperfection of a real measurement system are likely the dominant factors determining the practical limit of the enhancement effect. Nonetheless, to experimentally verify that there clearly exists an *intrinsic upper limit* in the QNPD enhancement effect as shown in Eqs. (28) and (29), we investigated the influence of the homodyne signal contribution ($|E_{\rm chiral}|^2$) on the chiroptical enhancement. Figure 4(a) depicts the standard deviation ($\sigma_s$) of the normalized ORD signal ($g/G$) as a function of $\beta$ to compare the ORD enhancement effects at low (24 mM) and high (120 mM) concentrations. Note that the homodyne signal intensity ($\propto |x|^2$) is determined by the chiroptical susceptibility ($\Delta\chi$), concentration ($c$), and path length ($L$) of the sample. Here, the total number of average photons [$N = (N^+ + N^-)/2$, where $N^{\pm}$ is the detected photon number of $I^{\pm}$] was controlled to be fixed so that the average intensity $(I^+ + I^-)/2$ read by the detector is constant regardless of varying $\beta$. However, the fixed $N$ values were differently set for 24 mM ($N = 250$) and 120 mM ($N = 1000$) because of the technical problem of the limited extinction ratio of our polarizer as follows. For the high concentration (120 mM), the homodyne signal intensity itself is strong enough to have $N = 1000$ constantly over the entire range of $\beta$. For the low concentration (24 mM), however, the incident beam intensity should be significantly increased to maintain $N = 1000$ at the very small $\beta$. Due to the limited extinction ratio (~ $10^{-5}$) of our polarizer, increasing the beam intensity inevitably produces non-negligible leaked light, which contaminates the $S_{\perp}$ signal and interferes with accurate measurements. To avoid this problem, $N = 250$ for 24 mM was chosen, where no significant contribution of the leaked light was observed even at $\beta$=0.14° which is the smallest $\beta$ accessible in our experiment.

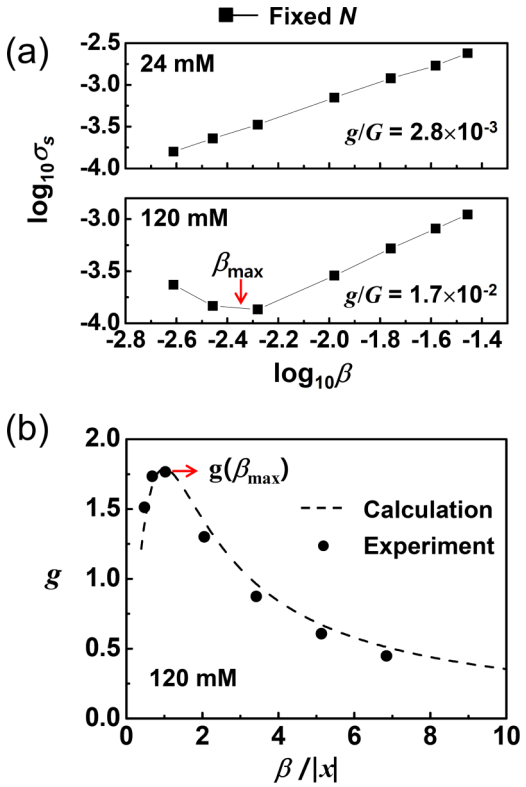


FIG. 4. (Color online) The chiroptical signal enhancement for fixed average photon counts ($N$). (a) The standard deviations ($\sigma_s$) of the normalized ORD signal ($g/G$) measured at 24 mM ($N = 250$) and 120 mM ($N = 1000$) concentrations of Ni(+) (tartrate)$_2$. (b) The measured ORD dissymmetry factor $g$ (circles) from Eq. (12) together with the calculated one (dashed line) from Eqs. (26) and (27), where $\mathrm{Re}[x] = \eta L/4 = -2.3 \times 10^{-3}$, $\mathrm{Im}[x] = \delta L/2 = 4.6 \times 10^{-3}$ and $|x| = 5.1 \times 10^{-3}$ were used in 120 mM Ni(+) (tartrate)$_2$.

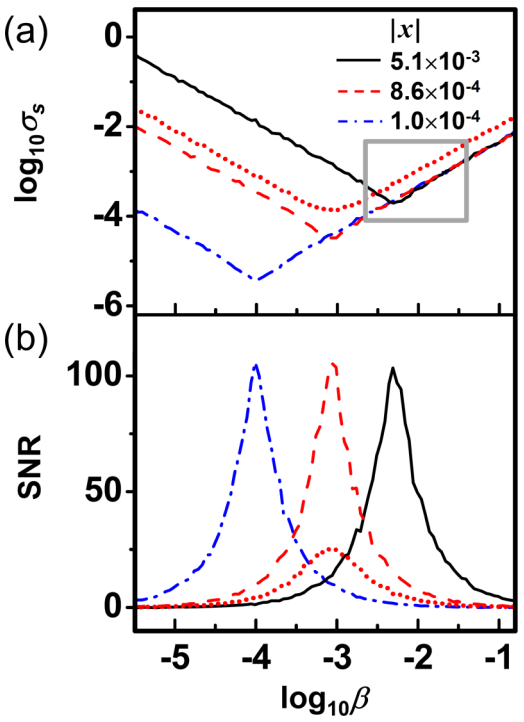


FIG. 5. (Color online) Numerical simulations of the chiroptical signal enhancement in the QNPD scheme. (a) The standard deviation ($\sigma_s$) and (b) SNR of the normalized ORD signal ($g/G$) as a function of $\beta$ for three different original chiroptical strengths, $|x| = 5.1 \times 10^{-3}$ (black solid line), $8.6 \times 10^{-4}$ (red dashed line), and $1.0 \times 10^{-4}$ (blue dash-dotted line). Fixed average photon counts ($N = 1000$) were used for all cases. For comparison with the experiment, the simulation results (red dotted line) at $N = 250$ are plotted for $|x| = 8.6 \times 10^{-4}$. The grayed square in (a) shows the measurement window in our experiment [see Fig. 4(a)].

In both cases, the SNR (inversely proportional to $\sigma_s$) improves as $\beta$ decreases as long as $\beta > \beta_{\max}$ while the $\sigma_s$ at 120 mM ($N = 1000$) is slightly smaller than that at 24 mM ($N = 250$) because the smaller is $N$, the lower is the SNR obtained in $I^{\pm}$. At the high concentration (120 mM), $\sigma_s$ has a minimum value at $\beta_{\max} \sim 4.5 \times 10^{-3}$ (maximum enhancement) and then increases again below that point. In contrast, such a minimum was not observed at the low concentration (24 mM) because the maximum enhancement is achieved at much smaller $\beta$ than the experimentally measurable range of $\beta$ (see the simulation results in Fig. 5).

Figure 4(b) depicts the enhanced ORD dissymmetry factor ($g$) with respect to $\beta/|x|$ for the high-concentration solution (120 mM) with $|x| = 5.1 \times 10^{-3}$. The dissymmetry factor $g$ reaches its maximum value $g(\beta_{\max}) = 1.77$ at $\beta_{\max} = 5.1 \times 10^{-3}$. The maximum enhancement factor is then estimated to be $G_{\max} = g(\beta_{\max})/g_{45} = 96.2$. This experimental result is in excellent agreement with the theoretically calculated value of $G_{\max} = 1/2|x| = 98.0$, indicating that $G_{\max}$ is indeed determined by the sample's original chiroptical intensity ($|x|$).

To further examine the dependence of the chiroptical enhancement on the original chiroptical strength ($|x|$), simple numerical simulations (see Fig. 5) of the ORD measurements with the QNPD method were carried out. Figure 5(a) shows the simulated standard deviations ($\sigma_s$) of the normalized ORD signals for three different chiroptical strengths ($|x| = 5.1 \times 10^{-3}$, $8.6 \times 10^{-4}$, and $1 \times 10^{-4}$). Here, the total number of average photons was set to be constant ($N = 1000$) irrespective of $\beta$. In the case of $|x| = 8.6 \times 10^{-4}$, an additional simulation of $N = 250$ (red dotted line) was performed for direct comparison with the experiment [compare Fig. 4(a) and the grayed square in Fig. 5(a)]. For all cases, the logarithm plots of $\sigma_s$ versus $\beta$ are V-shaped and show the minimum $\sigma_s$ (the best SNR) at each different $\beta_{\max}$. For $\beta > \beta_{\max}$, $\sigma_s$ decreases with $\beta$ due to the chiroptical enhancement effect ($G \sim 1/\beta$) but it increases again for $\beta < \beta_{\max}$ because the homodyne signal intensity ($|E_{\mathrm{chiral}}|^2$) contributes as a dominant noise source ($G \sim \beta$). $\beta_{\max}$ shifts to lower values ($\beta_{\max} = 5.1 \times 10^{-3}$, $8.6 \times 10^{-4}$, and $1.0 \times 10^{-4}$) as the original chiroptical strength $|x|$ becomes smaller; the results are in excellent agreement with the theoretical $\beta_{\max} = |x|$.

In both the experiment and numerical simulation above, the fixed average photon counts were used regardless of varying $\beta$. This is mainly to examine the existence of the enhancement limit intrinsically caused by the QNPD optical geometry in the ideal case. In a real measurement system, however, due to the finite detection sensitivity (or finite incident light

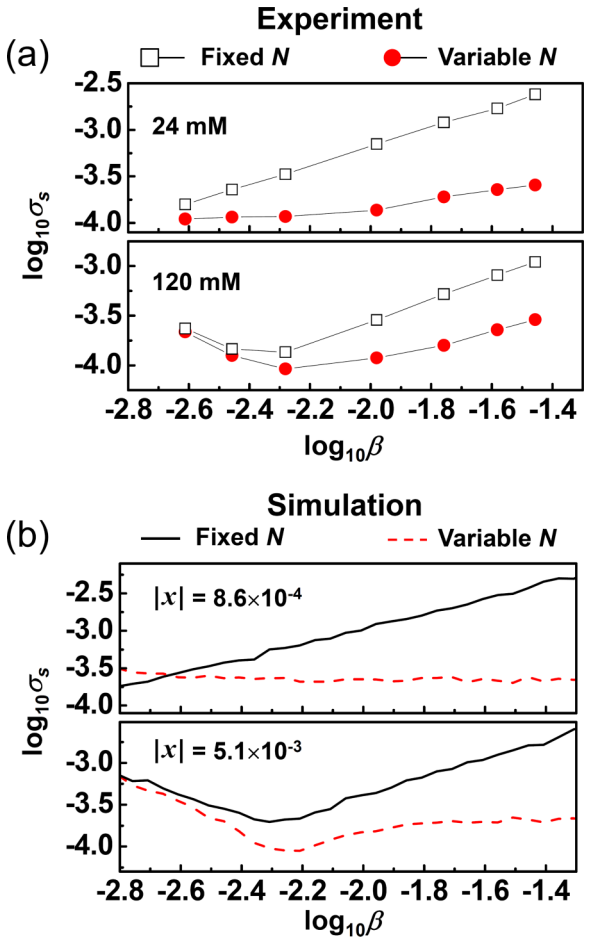


FIG. 6. (Color online) Comparison between the chiroptical enhancement effects for fixed and variable photon counts ($N$). The (a) experimentally measured and (b) simulated standard deviations ($\sigma_s$) of the normalized ORD signals for weak (24 mM and $|x| = 8.6 \times 10^{-4}$) and strong (120 mM and $|x| = 5.1 \times 10^{-3}$) chiroptical signal intensities. Fixed $N$: $N = 250$ at 24 mM and $|x| = 8.6 \times 10^{-4}$ and $N = 1000$ at 120 mM and $|x| = 5.1 \times 10^{-3}$. Variable $N$: (a) $N$ =46 000 and (b) $N$ =50 000, respectively, at $\beta$ =0.035.

intensity $\sim |E^0|^2$), keeping the number of the detected photons ($N$) constant as in the above case is not possible below very small $\beta$. Consequently, $N$ should decrease with $\beta$ ($I^{\pm} \sim |\sin\beta|^2|E^0|^2$).

Figure 6 shows how the enhancement effect is affected when the number of detected photons ($N$) varies with $\beta$. For comparison, the experimental and simulation results for fixed $N$ in Figs. 4(a) and 5(a) are plotted together [squares in Fig. 6(a) and solid line in Fig. 6(b)]. In both cases (24 mM and 120 mM), the standard deviations of the normalized ORD signals for variable $N$ are smaller than those for fixed $N$ at the largest $\beta$ ($\beta_i$ =0.035) in our experiment. This is because $N$ at $\beta_i$ ($N_i$) was differently set for each case in our experiment, i.e., $N_i$ (fixed)= 250 or 1000 and $N_i$ (variable)= 46 000. A stark contrast with the case of fixed $N$ (black squares) is that the enhancement effect at 24 mM is hardly observed for variable $N$ (red circles). Similarly in the case of 120 mM, the enhancement rate of $\beta$ for variable $N$ is significantly reduced at $\beta > \beta_{\max}$ in comparison to the case of fixed $N$ even though the minimum $\sigma_s$ in both cases appears at the same $\beta_{\max} = 5.1 \times 10^{-3}$. The lower enhancement observed at $\beta > \beta_{\max}$ for variable $N$ may originate from the decrease of the SNR by loss of detectable photons. In general, the SNR of detected photons ($N$) is simply given by $N/\sqrt{N} = \sqrt{N}$, assuming that the photon counting follows the Poisson distribution. Since the detected $N$ of $I^{\pm}$ is proportional to $\beta^2$ ($I^{\pm} \sim |\sin\beta|^2|E^0|^2 \propto \beta^2$) at small $\beta$, the SNR of photon loss decreases by a factor of $\beta$, which essentially cancels out with the enhancement effect $G \sim 1/\beta$. The simulation results in Fig. 6(b) also illustrate similar aspects. For variable $N$ (red dashed line), $\sigma_s$ does not change with $\beta$ at $\beta \gg \beta_{\max} = |x|$ so that there is no enhancement effect, which is in contrast with the case of fixed $N$ (black solid line) obeying $1/\beta$ enhancement. Therefore, a prior condition for making an effective chiroptical enhancement in the QNPD is that the total amount of signal photons should be kept constant without being reduced by $\beta$ to achieve the best SNR of the ORD signal ($g$).

## V. DISCUSSION

As mentioned earlier, the heterodyned term ($2\mathrm{Re}[E_{\mathrm{chiral}}E^*_{\mathrm{LO}}]$) produced by self-interference between $E_{\mathrm{chiral}}$ and $E_{\mathrm{LO}}$ determines the phase (sign) and amplitude of the chiroptical signal ($E_{\mathrm{chiral}}$) with respect to the homodyne terms ($|E_{\perp}|^2 + |E^{\pm}_{\mathrm{LO}}|^2$), which can be considered as positive background noise. The key to the chiroptical enhancement is to make the ratio of the heterodyne (signal) to the homodyne (noise) terms large, as shown in Eq. (24). In the QNPD scheme for ORD measurement, it is possible to increase this ratio simply by making the rotation angle $\phi$ small. At relatively large $\beta$ ($>\beta_{\max}$), $|E_{\mathrm{chiral}}| \ll |E_{\mathrm{LO}}|$ and the LO intensity is the main background noise ($|E_{\mathrm{chiral}}|^2 + |E_{\mathrm{LO}}|^2 \cong |E_{\mathrm{LO}}|^2$). Since this LO intensity is proportional to $|\sin\phi|^2$, the background noise is reduced as $\phi$ decreases. On the other hand, the chiral signal field strength is nearly unchanged because it is given by the product of the vertical field component of the incident slightly rotated LPL and the original chiroptical strength, i.e., $|E_{\mathrm{chiral}}| \propto |x||\cos\phi| \cong |x|$. Consequently, the chiral signal-to-noise ratio is given as $|E_{\mathrm{chiral}}|/|E_{\mathrm{LO}}| \cong |x|/|\phi|$ at small but not too small $\phi$.

As $\beta$ decreases further so that $|E_{\mathrm{chiral}}| \gg |E_{\mathrm{LO}}|$, the homodyne chiroptical signal is now the dominant noise source ($|E_{\mathrm{chiral}}|^2 + |E_{\mathrm{LO}}|^2 \cong |E_{\mathrm{chiral}}|^2$). Consequently, the enhanced dissymmetry factor ($g$) is decreased and vanishes as $\beta$ approaches zero. At perfect cross-polarization geometry ($\beta = 0$), the transmitted field intensity is solely from the homodyne chiroptical signal, i.e., $I^{\pm} = |E_{\mathrm{chiral}}|^2$. In this case, one cannot obtain any chiroptical information ($g = 0$) because the heterodyne term is zero ($2\mathrm{Re}[E_{\mathrm{chiral}}E^*_{\mathrm{LO}}] = 0$) so that the phase information of $E_{\mathrm{chiral}}$ is completely lost in the observables ($I^{\pm}$).

### A. Imperfect polarizer

In our QNPD setup, the maximum ORD enhancement ($G \sim 400$) at 3 mM concentration was obtained at $\beta = 1.7 \times 10^{-3}$ (see Fig. 3). This enhancement factor is however much smaller than the theoretical upper limit $G_{\max} \cong 1/2|x| = 3100$. One of the determining factors is optical imperfection of the prism-type polarizer (Glan-Laser or

Glan-Thomson polarizer) used here. Due to the nonzero extinction ratio ($\rho_e \sim 10^{-5}$) of the polarizers, undesired transmitted light passing through the crossed polarizer-analyzer was detected at $\beta < 1.7 \times 10^{-3}$. This ($\sim 10^{-5}|E^0|^2$, where $|E^0|$ is the incident beam amplitude) becomes the dominant noise source because it is even larger than the LO intensity ($|\sin\beta|^2|E^0|^2 \sim 2.9 \times 10^{-6}|E^0|^2$ at $\beta = 1.7 \times 10^{-3}$). Consequently, the transmitted light due to imperfect polarizers makes the experimentally achievable enhancement factor smaller than the ideal limit. Clearly, use of polarizers with better extinction ratio such as a Brewster angle reflection polarizer ($\rho_e \sim 10^{-7}$) [17,18] would enable one to reach as close to the intrinsic enhancement limit ($G_{\max} = 3100$ in the present case) as possible.

### B. Detector sensitivity

Finite detection sensitivity of real detectors could also be another practical problem limiting the effective enhancement. At relatively large $\beta$, the transmitted intensity ($I^{\pm}$) is strong enough so that a light intensity attenuator should be used in front of the detector to avoid detector saturation as well as to achieve a good SNR. At very small $\beta$, however, the transmitted intensity level ($\sim|\sin\beta|^2|E^0|^2$) could be too low to make the total amount of detected photons constant for maintaining the best SNR even with a highly sensitive detector. In our case, the incident light power (>500 mW at 800 nm) is high enough to saturate the CCD detector even at $\beta = 1.7 \times 10^{-3}$. Therefore, it is the low extinction ratio of the polarizers instead of the limited detection sensitivity that is the dominant factor preventing us from realizing the ideal enhancement of the chiroptical measurement. However, for vibrational optical activity (VOA) measurement in the IR frequency range, the detection sensitivity would be critical not only because the VOA signal is exceedingly small ($|x| \sim 10^{-5}$) but also because both the IR detector and IR light source are less sensitive and weaker, respectively, than those in the visible frequency domain. Noting that the intrinsic maximum enhancement factor is purely determined by the original chiroptical intensity ($G_{\max} \cong 1/2|x|$), we believe that the potentially achievable enhancement for the VOA signal is much larger than that of the electronic counterpart. However, since $\beta_{\max}(=|x|)$ giving $G_{\max}$ becomes much smaller along with the very small $|x|$ value and the transmitted light level at $\beta_{\max}$ is likely to be extremely weak ($\sim |\sin\beta_{\max}|^2|E^0|^2$), the detector sensitivity or the incident light intensity would be a critical factor for achieving maximal enhancement in the VOA measurement.

### C. Comparison with previous works

The enhancement effects on chiroptical measurements with the QNPD method were briefly discussed in our recent review article [15]. However, it appears that the presence of intrinsic upper limits of such chiroptical enhancement effects has not been discussed nor experimentally demonstrated before. Therefore, before we close this section, we shall compare how these chiroptical enhancement effects are related to other previous works.

Recently, a direct connection between the QNPD enhancement effects in chiroptical spectroscopy and the weak amplifications with the cross-polarizer method has been revealed and discussed [19]. For the sake of completeness, let us briefly discuss the essential aspect of weak measurement theory. The Hamiltonian of the standard measurement is written as $\hat{H} = -\alpha x' \hat{A}$, where $x'$ is a canonical variable of the meter and $\alpha$ is either unity or a normalized time-dependent function compactly centered at the time of measurement. Considering an ensemble of photons in an optical measurement, with a *preselected* initial state $|\psi_i\rangle$ and a *postselected* final state $|\psi_f\rangle$ with $|g(x')\rangle$ the initial state of the measuring device, Aharonov, Albert, and Vaidman showed that the probability amplitude can be approximately given as [20]

$$\begin{aligned}\langle\psi_f|\Psi\rangle &= \langle\psi_f|e^{-i\int\hat{H}(t)dt}|g(x')\rangle|\psi_i\rangle \\ &\cong \langle\psi_f|1 - i\int\hat{H}(t)dt|g(x')\rangle|\psi_i\rangle \\ &= \langle\psi_f|\psi_i\rangle(1 - ix'A_w)|g(x')\rangle \\ &\cong \langle\psi_f|\psi_i\rangle e^{-ix'A_w}|g(x')\rangle, \end{aligned} \tag{30}$$

where the weak value of the system operator $\hat{A}$ is defined as

$$A_w \equiv \frac{\langle\psi_f|\hat{A}|\psi_i\rangle}{\langle\psi_f|\psi_i\rangle}. \tag{31}$$

Then it was shown that the weak value in Eq. (31) can be arbitrarily large, far outside the range of eigenvalues of $\hat{A}$, if the overlap $\langle\psi_f|\psi_i\rangle$ between the pre- and postselected states or the detection probability $|\langle\psi_f|\psi_i\rangle|^2$ is made to be very small. Experimentally, this is realized by controlling the transmission axes of the polarizer and the analyzer to be orthogonal to each other, and this weak value amplification scheme has been applied to measurements of the phase and amplitude of the photon wave function [21], polarization-state-dependent beam deflection of 1 Å [22], and the small longitudinal phase shift induced by birefringent materials [23]. In fact, these optical measurements with cross polarizer-analyzer geometry are essentially identical to the present QNPD method, which was initially shown to be of use by Kliger [5,6]. In the case of the present QNPD chiroptical measurement, using the linearization-and-exponentiation approximation in Eq. (30) and considering the chiral-medium influence operator $e^{-i\hat{A}_c L}$, with $\hat{A}_c$ in Eq. (2), one can show that the $H$ component of the transmitted light after its interaction with the chiral medium is given as, for ($\pm$) EPL used to measure the CD signal, $E_H^{\pm} \cong \pm i|E_H^0|\,e^{-iA_{w,\mathrm{EPL}}^{\pm}L}$, and ($\pm$)-rotated LPL used to measure the ORD (or circular birefringence) signal, $E_H^{\pm} \cong \pm|E_H^0|\,e^{-iA_{w,\mathrm{rLPL}}^{\pm}L}$, where the corresponding chiroptical weak values are, respectively,

$$A_{w,\mathrm{EPL}}^{\pm} \equiv \frac{\langle H|\hat{A}_c|\psi^{\pm}\rangle}{\langle H|\psi^{\pm}\rangle} = \left(\rho \mp \frac{\delta}{2}\frac{1}{\beta}\right) - i\left(\frac{\kappa}{2} \mp \frac{\eta}{4}\frac{1}{\beta}\right) \tag{32}$$

and

$$A_{w,\mathrm{rLPL}}^{\pm} \equiv \frac{\langle H|\hat{A}_c|\psi^{\pm}\rangle}{\langle H|\psi^{\pm}\rangle} = \left(\rho \mp \frac{\eta}{4}\frac{1}{\beta}\right) - i\left(\frac{\kappa}{2} \pm \frac{\delta}{2}\frac{1}{\beta}\right), \tag{33}$$

where the corresponding aspect ratios are defined in Eqs. (14) and (25). Again, in the limit of small elliptical angle of

EPL or rotation angle of LPL used to measure CD and ORD, respectively, the amplification factors both are $1/\beta$ so that as the ellipticity angle $\theta$ or rotation angle $\phi$ decreases, the corresponding dissymmetry factors for CD and ORD signals increase, i.e., there is an amplification effect. However, as shown in this paper, the amplification factor cannot be arbitrarily large due to the intrinsic contribution from the homodyne term [see Eqs. (13) and (24)].

This existence of an upper limit in the QNPD enhancement factor is, in fact, similar to the case of the enhancement effect of the so-called superchiral field on optical enantioselectivity [14,15,24]. Tang and Cohen [25,26] considered the dissymmetry factor for optical enantioselectivity defined as

$$g = \frac{A^+ - A^-}{(A^+ + A^-)/2}, \tag{34}$$

where $A^\pm$ are the rates of absorption of $(\pm)$-handed chiral light by a given chiral molecule. Since $A^\pm$ can be written as a sum of chiral and nonchiral terms as $A^\pm = A_{\text{nonchiral}} \pm A_{\text{chiral}}$, the dissymmetry factor for optical enantioselectivity is

$$g = \frac{2A_{\text{chiral}}}{A_{\text{nonchiral}}} \tag{35}$$

where

$$A_{\text{nonchiral}} \cong \frac{2\omega}{\varepsilon_0}\left(\alpha'' U_e + \frac{1}{c^2}\chi'' U_m\right) \tag{36}$$

and

$$A_{\text{chiral}} = -\frac{2}{\varepsilon_0} G' C. \tag{37}$$

Here, the imaginary parts of the complex electric polarizability and the complex magnetic susceptibility are denoted as $\alpha''$ and $\chi''$, respectively. $G'$ represents the real part of the mixed electric-dipole–magnetic-dipole polarizability $\tilde{G}$, which is a measure of molecular chirality, whereas the $C$ factor defined as $(1/2)\varepsilon_0\{\boldsymbol{E}\cdot(\nabla\times\boldsymbol{E}) + c^2\boldsymbol{B}\cdot(\nabla\times\boldsymbol{B})\}$ is a measure of optical chirality [25,27]. The electric and magnetic field energy densities are denoted as $U_e$ and $U_m$, respectively, in Eq. (36).

For traveling plane-polarized light waves, the electric-field—electric-dipole interaction strength is two to three orders of magnitude larger than the magnetic-field—magnetic-dipole interaction strength, i.e., $\alpha'' U_e \gg \chi'' U_m/c^2$. Therefore, the second term in the expression for $A_{\text{nonchiral}}$ in Eq. (36) can be safely ignored. In addition to this approximation, Tang and Cohen further considered standing-wave-type chiral fields with nodes at which the electric field energy density approaches zero. Consequently, it was shown that the dissymmetry factor in this special case can be arbitrarily large, i.e.,

$$g \propto (C/U_e) \to \infty \quad \text{as} \quad U_e \to 0. \tag{38}$$

However, due to the fact that the total electromagnetic field energy density does not depend on position, the approximation $\alpha'' U_e \gg \chi'' U_m/c^2$ may not hold at the nodes of electric field. In the region where $\alpha'' U_e < \chi'' U_m/c^2$, the dissymmetry factor decreases and approaches zero as $U_e \to 0$ [14]. Therefore, there should exist an intrinsic limit in the enhancement of $g$ for optical enantioselectivity, much like the existence of an intrinsic limit in the enhancement factor for QNPD chiroptical spectroscopy.

To make this analogy clear, let us consider the terms contributing to $A_{\text{nonchiral}}$ and $A_{\text{chiral}}$ in more detail. From the Fermi's golden rule expression, the first term $2\omega\alpha'' U_e/\varepsilon_0$ in $A_{\text{nonchiral}}$ results from the interaction between the electric field and the electric-field-induced electric dipole, whereas the second term $2\omega\chi'' U_m/(\varepsilon_0 c^2)$ results from the interaction between the magnetic field and the magnetic-field-induced magnetic dipole. However, $A_{\text{chiral}}$ represents the transition probability induced by mixed interactions between the electric field and the magnetic-field-induced electric dipole and between the magnetic field and the electric-field-induced magnetic dipole. Therefore, the two terms contributing to $A_{\text{nonchiral}}$ can be considered as homo-transition processes, and those contributing to $A_{\text{chiral}}$ as hetero- (mixed-) transition processes. Similarly to the fact that the chiroptical enhancement factor reaches its maximum value when the two homodyne terms have an equal magnitude, i.e., $|E_{\text{chiral}}| = |E_{\text{LO}}|$ in Eqs. (13) and (24), the enhancement factor for optical enantioselectivity was shown to be maximum at $\alpha'' U_e = \chi'' U_m/c^2$. This equality suggests that the maximum enhancement of any optical enantioselectivity is expected when the ratio of the electric field and magnetic field energy densities is controlled to be the ratio of the magnetic and electric susceptibilities, i.e., $U_e/U_m = \chi''/c^2\alpha''$.

Recently, Cameron and Barnett [28] showed that the dissymmetry factor for Raman optical activity (ROA) can be arbitrarily large when chiral molecules are placed at the nodal regions of the standing-wave-type chiral fields that were originally considered by Tang and Cohen. They showed that the enhancement effect becomes very large as the electric field energy density approaches zero. However, their results were based on the same approximation that the electric-field—electric-dipole interaction strength is two to three orders of magnitude larger than the magnetic-field—magnetic-dipole interaction strength. Again, this is valid only for traveling-wave-type chiral fields and not for standing-wave-type chiral fields so that there should also exist an intrinsic upper limit in the enhancement effect on the ROA by the superchiral field. This is currently under investigation and the result will be presented elsewhere.

## VI. SUMMARY AND A FEW CONCLUDING REMARKS

In this paper, the underlying enhancement mechanism of a chiroptical measurement combined with heterodyned detection in the QNPD method was fully elucidated and the intrinsic limitations of such enhancement effects in CD and ORD measurements with EPL and rotated LPL, respectively, were clarified. It was demonstrated that the ORD dissymmetry factor ($g$) can be significantly enhanced by adjusting the rotation angle of the incident LPL in the QNPD method but there exists an intrinsic upper limit, which is purely determined by the original chiroptical strength ($|x|$) of the sample. For an originally weak ORD signal ($|x| = 1.6 \times 10^{-4}$), however, its amplification was experimentally limited to ~400 times, which is far from its ideal limit ($G_{\max} \cong 1/2|x| = 3100$) and is thus considered as the practical limit caused by other technical problems. Although the primary source limiting the enhancement effect observed in our QNPD setup is the

low extinction ratio of real polarizers used, the intrinsic enhancement limit is mainly due to the homodyne chiroptical intensity contribution to the corresponding dissymmetry factor regardless of the imperfection of a real measurement system. With more optically perfect polarizers and a stronger light source, we believe that a higher amplification toward the intrinsic limit would be achievable in the QNPD method.

## ACKNOWLEDGMENTS

This work was supported by the Korea Basic Science Institute (KBSI Grant No. T34428) for H.R. The experimental data presented here were measured using the Femtosecond Multidimensional Laser Spectroscopic System (FMLS) at KBSI. M.C. is grateful for the financial support by Grant No. IBS-R023-D1.

[1] N. Berova, K. Nakanishi, and R. W. Woody, *Circular Dichroism: Principles and Applications*, 2nd ed. (Wiley-VCH, New York, 2000).
[2] L. D. Barron, *Molecular Light Scattering and Optical Activity*, 2nd ed. (Cambridge University Press, Cambridge, UK, 2004).
[3] L. A. Nafie, *Vibrational Optical Activity: Principles and Applications* (Wiley, Chichester, UK, 2011).
[4] E. Chen, Y. Wen, J. W. Lewis, R. A. Goldbeck, D. S. Kliger, and C. E. M. Strauss, Rev. Sci. Instrum. **76**, 083120 (2005).
[5] D. B. Shapiro, R. A. Goldbeck, D. Che, R. M. Esquerra, S. J. Paquette, and D. S. Kliger, Biophys. J. **68**, 326 (1995).
[6] C. F. Zhang, J. W. Lewis, R. Cerpa, I. D. Kuntz, and D. S. Kliger, J. Phys. Chem. **97**, 5499 (1993).
[7] J. Helbing and M. Bonmarin, J. Chem. Phys. **131**, 174507 (2009).
[8] I. Eom, S.-H. Ahn, H. Rhee, and M. Cho, Phys. Rev. Lett. **108**, 103901 (2012).
[9] H. Rhee, I. Eom, S.-H. Ahn, and M. Cho, Chem. Soc. Rev. **41**, 4457 (2012).
[10] H. Rhee, Y.-G. June, J.-S. Lee, K.-K. Lee, J.-H. Ha, Z. H. Kim, S.-J. Jeon, and M. Cho, Nature (London) **458**, 310 (2009).
[11] I. Eom, S.-H. Ahn, H. Rhee, and M. Cho, Opt. Express **19**, 10017 (2011).
[12] K. Hiramatsu, H. Kano, and T. Nagata, Opt. Express **21**, 13515 (2013).
[13] K. Hiramatsu, M. Okuno, H. Kano, P. Leproux, V. Couderc, and Hiro-o Hamaguchi, Phys. Rev. Lett. **109**, 083901 (2012).
[14] J. S. Choi and M. Cho, Phys. Rev. A **86**, 063834 (2012).
[15] H. Rhee, J. S. Choi, D. J. Starling, J. C. Howell, and M. Cho, Chem. Sci. **4**, 4107 (2013).
[16] S. R. Domingos, A. Huerta-Viga, L. Baij, S. Amirjalayer, D. A. E. Dunnebier, A. J. C. Walters, M. Finger, L. A. Nafie, B. Bruin, W. J. Buma, and S. Woutersen, J. Am. Chem. Soc. **136**, 3530 (2014).
[17] D. J. Dummer, S. G. Kaplan, L. M. Hanssen, A. S. Pine, and Y. Zong, Appl. Opt. **37**, 1194 (1998).
[18] H. Rhee, S.-S. Kim, S.-J. Jeon, and M. Cho, ChemPhysChem **10**, 2209 (2009).
[19] M. Cho, Phys. Rev. A **88**, 023833 (2013).
[20] Y. Aharonov, D. Z. Albert, and L. Vaidman, Phys. Rev. Lett. **60**, 1351 (1988).
[21] J. S. Lundeen, B. Sutherland, A. Patel, C. Stewart, and C. Bamber, Nature (London) **474**, 188 (2011).
[22] O. Hosten and P. Kwiat, Science **319**, 787 (2008).
[23] N. Brunner and C. Simon, Phys. Rev. Lett. **105**, 010405 (2010).
[24] K. Y. Bliokh and F. Nori, Phys. Rev. A **83**, 021803(R) (2011).
[25] Y. Tang and A. E. Cohen, Phys. Rev. Lett. **104**, 163901 (2010).
[26] Y. Tang and A. E. Cohen, Science **332**, 333 (2011).
[27] R. P. Cameron, S. M. Barnett, and A. M. Yao, New J. Phys. **14**, 053050 (2012).
[28] R. P. Cameron and S. M. Barnett, Phys. Chem. Chem. Phys. **16**, 25819 (2014).